Journal of Organometallic Chemistry 750 (2014) 169–175

Contents lists available at ScienceDirect

Journal of Organometallic Chemistry

journal homepage: www.elsevier.com/locate/jorganchem

Ruthenium(II) complexes derived from the ligands having carboxamide groups: Reactivity and scavenging of nitric oxide (NO)

Kaushik Ghosh*, Sushil Kumar, Rajan Kumar, Udai P. Singh

Department of Chemistry, Indian Institute of Technology, Roorkee, Roorkee 247667, Uttarakhand, India

ARTICLE INFO

Article history:
Received 30 July 2013
Received in revised form
26 October 2013
Accepted 29 October 2013

Dedicated to Professor R. N. Mukherjee on his 60th birthday.

Keywords:
Ruthenium complex
Carboxamide group
Metal redox
Nitric oxide (NO)
NO scavenging

ABSTRACT

Two novel ruthenium(II) complexes $[Ru^{II}(L^1)(PPh_3)_2(CO)]$ (**1**) and $[Ru^{II}(L^3)(PPh_3)_2(DMF)]$ (**2**) derived from the carboxamide ligands L^1H_2 and L^2H_2 respectively (where L^1H_2 = N^2,N^6-di*p*-tolylpyridine-2,6-dicarboxamide and L^2H_2 = N^2,N^6-di(naphthalen-1-yl)pyridine-2,6-dicarboxamide) were synthesized and characterized. Molecular structures of complexes **1**·CH_3OH and **2**·DMF were authenticated using X-ray crystallographic studies. Both the complexes were characterized using IR, UV–vis, elemental analysis, NMR and ESI-mass spectral studies. Electrochemical studies were performed to investigate the redox properties. Nitric oxide (NO) scavenging activity of these complexes was also observed with the help of Griess reagent reaction.

1. Introduction

Coordination chemistry of metal complexes derived from the ligands containing carboxamide (–CONH–) nitrogen donors has received considerable current attention [1–7]. There are several roles exhibited by carboxamide nitrogen in the chemistry of different coordination complexes. For example, cobalt and iron centers present in the enzyme nitrile hydratase (NHase) are bound through carboxamido nitrogen atoms [8–10]. This amido nitrogen possessing *trans effect* is also found to be important for the coordination and photolability of nitric oxide (NO) [11–14]. The binding of two carboxamido nitrogen atoms with copper center was observed in prion protein [7]. Collins and coworkers [5,6] have extensively studied the coordination chemistry of metal complexes derived from the macrocyclic ligands containing four carboxamido nitrogen donor centers.

As a part of our ongoing research we are trying to synthesize ruthenium nitrosyl complexes having $\{RuNO\}^6$ moiety [15–20]. We would like to mention here that nitric oxide (NO) exhibits concentration dependent activities in biosystem [16]. Hence, biological targets having NO deficiency would need NO-donors whereas scavenging of NO is necessary during overproduction of NO. NO is known to be a π-acid ligand and this ligand will prefer to bind to a metal center in lower oxidation state(s) like Ru(II) rather than Ru(III). However, Ru(II) center will provide complex having $\{RuNO\}^7$ moiety (according to the Enemark and Feltham notation) [18] after reacting with NO. Investigation of literature [15–20] predicted that nitrosyl complex having $\{RuNO\}^6$ species is more stable than the complex having $\{RuNO\}^7$ moiety. Complexes with $\{RuNO\}^7$ moiety could undergo oxidation and ruthenium nitrosyl complexes having $\{RuNO\}^6$ moiety would be produced. Hence NO will react with Ru(II) center and will ultimately give rise to stable ruthenium complex having $\{RuNO\}^6$ moiety and NO will be scavenged. Although there are reports on the importance of scavenging of NO [21–24], literature on ruthenium complexes are scarce [23,24].

Hence in our synthetic strategy, we prepare Ru(III) complexes which would ultimately give rise to ruthenium nitrosyl complexes having $\{RuNO\}^6$ species. Carboxylates are well known hard donors [25] and stabilize higher oxidation states of metal ions and hence we have studied the chemistry of ruthenium(III) complexes derived from the ligands having mono- and di-carboxylate (–COO) groups [19,20] and their interaction with nitric oxide. It is well known in the literature that carboxamido nitrogens are strong σ-donor and stabilize the higher oxidation states of metal [2–6]. This prompted us to explore the chemistry of ligands containing carboxamido nitrogen donors L^1H_2 (N^2,N^6-di-*p*-tolylpyridine-2,6-dicarboxamide) and L^2H_2 (N^2,N^6-di-(naphthalen-1-yl)pyridine-2,6-dicarboxamide) (Scheme 1).

* Corresponding author. Fax: +91 1332 273560.
E-mail addresses: ghoshfcy@iitr.ernet.in, ghoshinorgchem@gmail.com (K. Ghosh).

0022-328X/$ – see front matter © 2013 Elsevier B.V. All rights reserved.
http://dx.doi.org/10.1016/j.jorganchem.2013.10.054

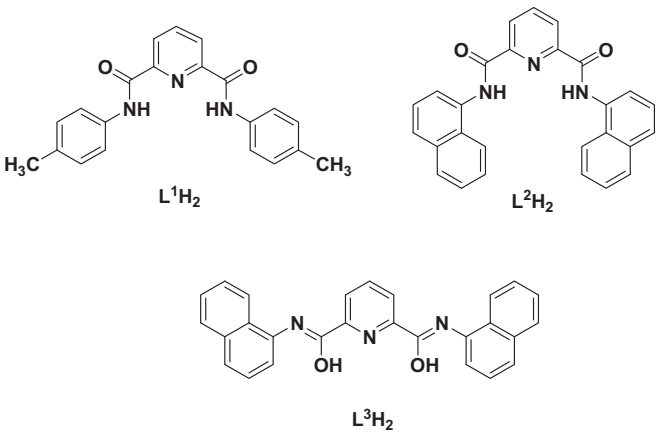

Scheme 1. Schematic drawings of the ligands used to prepare ruthenium complexes.

To the best of our knowledge, the reactivity of ligand containing carboxamide groups with $[Ru^{II}(PPh_3)_3Cl_2]$ has never been studied. Hence in the present report, we described the synthesis and characterization of ruthenium(II) complexes $[Ru^{II}(L^1)(PPh_3)_2(CO)]$ (**1**) and $[Ru^{II}(L^3)(PPh_3)_2(DMF)]$ (**2**) (shown in Scheme 2) derived from the reaction of $[Ru^{II}(PPh_3)_3Cl_2]$ with carboxamide ligands L^1H_2 and L^2H_2 respectively.

Molecular structures of complexes **1**·CH_3OH and **2**·DMF were determined using X-ray crystallographic studies. We have characterized the resultant complexes by IR, UV–vis, NMR and ESI-MS and redox properties were investigated by electrochemical studies. We have also investigated the nitric oxide reactivity studies on complexes **1** and **2**.

2. Experimental section

2.1. Reagents and materials

Analytical grade reagents pyridine-2,6-dicarboxylic acid, *para*-toluidine, 1-naphthyl amine, sulphanilamide and naphthylethylenediamine dihydrochloride (NED) (Himedia Laboratories Pvt. Ltd., Mumbai, India) were used as obtained. Double distilled water was used in all the experiments.

2.2. Physical measurements

The electronic absorption spectra were recorded in *N*,*N*′-dimethylformamide, methanol and acetonitrile solvents with an Evolution 600, Thermo Scientific UV–vis spectrophotometer. ESI-mass spectra for complexes **1** and **2** in methanolic solutions were recorded in the positive ion mode using Thermo Finnigan LCQ Deca mass spectrometer. Infrared spectra were obtained as KBr pellets with Thermo Nicolet Nexus FT-IR spectrometer, using 16 scans and were reported in cm^{-1}. ^1H and ^{31}P NMR spectra were recorded on Bruker AVANCE, 500.13 MHz spectrometer in the deuterated solvents.

2.3. Synthesis of ligand L^1H_2

A solution of pyridine-2,6-dicarboxylic acid (0.67 g, 4.0 mmol) in 15 mL of dry dimethylformamide was cooled on an ice bath and was stirred for 15 min. To this solution, 2.56 g (19.0 mmol) of 1-hydroxybenzotriazole (HOBT) and 1.96 g (9.5 mmol) of dicyclohexylcarbodiimide (DCC) were added and the mixture was stirred for another 0.5 h at 0 °C. Now a batch of *para*-toluidine 0.96 g (9.0 mmol) was added to the same reaction mixture with stirring for next 2 h on the same ice bath. After 2 h, the ice bath was removed and the stirring was continued overnight at room temperature. After the removal of white precipitate of *N*,*N*′-dicyclohexylurea by filtration, the solvent was evaporated and the residue was dissolved in 20 mL of ethyl acetate. The organic phase was washed twice with water (100 mL) and dried over anhydrous sodium sulfate (Na_2SO_4). The solvent was concentrated to 10 mL. Next day, a white crystalline solid of ligand L^1H_2 was settled down on the bottom of beaker which was filtered and was washed with ethyl acetate and diethyl ether. Yield: 0.84 g (61%). Anal. Calcd. for $C_{21}H_{19}N_3O_2$ (345.15): C, 73.03; H, 5.54; N, 12.17. Found: C, 72.98; H, 5.22; N, 12.67. IR (KBr disk, cm^{-1}): 1654 (ν_{CO}, –CONH), 3303 (ν_{N-H}) cm^{-1}. UV–vis (CH_3CN; λ_{max}, nm (ε, M^{-1} cm^{-1})): 289 (12,914). ^1H NMR ($(CD_3)_2SO$, 500 MHz): δ 10.96 (s, 2H), 8.38 (d, 2H), 8.28 (t, 1H), 7.79 (d, 4H), 7.25 (d, 4H), 2.32 (s, 6H) ppm.

2.4. Synthesis of ligand L^2H_2

Ligand L^2H_2 was synthesized using naphthyl amine and pyridine-2,6-dicarboxylic acid by following the same synthetic procedure as for ligand L^1H_2. Yield: 55%. Anal. Calcd. for $C_{27}H_{19}N_3O_2$ (417.15): C, 77.68; H, 4.59; N, 10.07. Found: C, 78.11; H, 4.92; N, 9.98. IR (KBr disk, cm^{-1}): 1659 (ν_{CO}, -CONH), 3302 (ν_{N-H}) cm^{-1}. UV–vis (CH_3CN; λ_{max}, nm (ε, M^{-1} cm^{-1})): 292 (13,900), 315 (11,150). ^1H NMR ($(CD_3)_2SO$, 500 MHz): δ 11.44 (s, 2H), 8.46 (d, 2H), 8.37 (t, 1H), 8.11 (d, 2H), 8.01 (d, 2H), 7.92 (d, 2H), 7.71 (d, 2H), 7.62–7.58 (m, 6H) ppm.

2.5. Synthesis of complex $[Ru^{II}(L^1)(PPh_3)_2(CO)]$ (**1**)

A solution of 0.15 mmol of ligand L^1H_2 (0.052 g) was prepared in 10 mL of *N*,*N*′-dimethylformamide and to it was added solid NaH (0.32 mmol, 0.008 g) to obtain a light yellow solution of deprotonated ligand. This mixture was added slowly to a hot solution of $Ru(PPh_3)_3Cl_2$ (0.1 mmol, 0.096 g) in methanol (20 mL). The reaction mixture was heated under reflux for 5–6 h. The brown color of the solution was turned to orange red. Slow evaporation of the solution mixture afforded orange red precipitate which was washed with methanol and diethyl ether. Single crystals of the complex **1** for X-

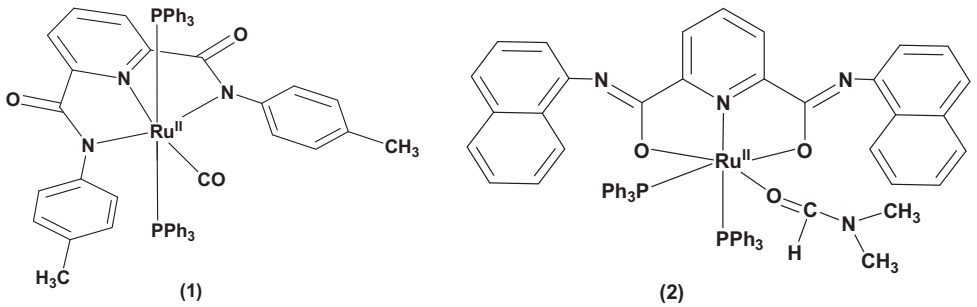

Scheme 2. Schematic drawings of ruthenium complexes $[Ru^{II}(L^1)(PPh_3)_2(CO)]$ (**1**) and $[Ru^{II}(L^3)(PPh_3)_2(DMF)]$ (**2**).

ray crystallography were obtained within three days upon slow evaporation of solution of **1** in methanol/DMF mixture (Yield: 48%). Anal. Calcd. for $C_{59}H_{51}N_3O_4P_2Ru$ (1029.24): C, 68.86; H, 5.00; N, 4.08. Found: C, 67.88; H, 4.99; N, 3.84. ESI-MS: *m/z* 997.9; $[Ru(L^1)(PPh_3)_2(CO)]^+$, *m/z* 736.0; $[Ru(L^1)(PPh_3)(CO)]^+$. IR (KBr disk, cm^{-1}): 1936 (ν_{CO}, carbon monoxide), 1672 (ν_{CO}, −CONH), 746, 694, 519 (ν_{PPh3}) cm^{-1}. UV–vis (CH_2Cl_2; λ_{max}, nm (ε, M^{-1} cm^{-1})): 246 (45,000), 314 (12,500), 415 (4700). ^1H NMR ($(CD_3)_2SO$, 500 MHz): δ 8.08 (d, 1H), 7.67 (d, 1H), 7.39–7.44 (m, 7H), 7.21–7.29 (m, 9H),7.12 (d, 3H), 7.05 (t, 3H), 6.94–6.99 (m, 10H), 6.82–6.89 (m, 5H), 6.63 (d, 1H), 6.55 (d, 1H), 2.32 (s, 6H) ppm. ^{31}P NMR ($(CD_3)_2SO$, 500 MHz): δ 21.48 ppm.

2.6. Synthesis of complex $[Ru^{II}(L^3)(PPh_3)_2(DMF)]$ (**2**)

To a benzene solution (15 mL) of $Ru(PPh_3)_3Cl_2$ (0.1 mmol, 0.096 g), a batch of ligand L^2H_2 (0.15 mmol, 0.062 g) with 10 mL of methanol was directly added. The reaction mixture was heated under reflux for 6 h and the color of the solution was turned from brown to red. The solvent was evaporated to obtain a red solid which was dissolved again in dichloromethane. Complex **2** (0.058 g, 0.052 mmol) was eluted on an alumina column by dichloromethane:acetonitrile (6:4) mixture. Single crystals of the complex **2** for X-ray crystallography were obtained within 2 days upon slow evaporation of the solution of compound in *N,N′*-dimethylformamide (Yield: 52%). Anal. Calcd. for $C_{69}H_{61}N_5O_4P_2Ru$ (1187.32): C, 69.80; H, 5.18; N, 5.90. Found: C, 69.71; H, 5.35; N, 5.98. ESI-MS: *m/z* 1042.03; $[Ru(L^3)(PPh_3)_2]^+$, *m/z* 780.11; $[Ru(L^3)(PPh_3)]^+$, *m/z* 518.23; $[Ru(L^3)]^+$. IR (KBr disk, cm^{-1}): 1672 (ν_{CO}, DMF), 745, 698, 524 (ν_{PPh3}) cm^{-1}. UV–vis (CH_2Cl_2; λ_{max}, nm (ε, M^{-1} cm^{-1})): 340 (14,839), 470 (4193). ^1H NMR (CD_3CN, 500 MHz): δ 8.31 (d, 2H), 8.07 (d, 2H), 7.95 (s, 1H), 7.91 (d, 2H), 7.86 (t, 1H), 7.70 (d, 2H), 7.61 (d, 2H), 7.56 (d, 2H), 7.49 (t, 2H), 7.38 (t, 2H), 7.17 (t, 3H), 7.12–7.08 (m, 9H), 6.93–6.89 (m, 12H), 6.79–6.76 (m, 6H), 2.91 (s, 3H), 2.80 (s, 3H) ppm. ^{31}P NMR (CD_3CN, 500 MHz): δ 50.60 and 42.68 ppm.

2.7. Griess reagent assay for NO scavenging activity

The NO scavenging activity of complexes **1** and **2** were performed using Griess reagent assay with sodium nitrite. The Griess reagent was prepared by mixing equal volumes of 1% sulphanilamide in 5% orthophosphoric acid and 0.1% naphthylethylenediamine dihydrochloride (NED) in distilled water. The amount of NO scavenged by **1** and **2** was measured by observing the decrease in the absorbance of produced dye at ~538 nm using UV–vis spectrophotometer.

2.8. X-ray crystallography

Orange red crystals of complex **1**, suitable for diffraction were grown via slow evaporation of solution of the compound in DMF/methanol mixture however the single crystals for **2** (red colored) were obtained via slow evaporation of solution of **2** in DMF. The X-ray data collection and processing for complexes were performed on Bruker Kappa Apex-II CCD diffractometer by using graphite monochromated Mo-Kα radiation ($\lambda = 0.71070$ Å) at 293 K for both the complexes. Crystal structures were solved by direct methods. Structure solutions, refinement and data output were carried out with the SHELXTL program [26,27]. All non-hydrogen atoms were refined anisotropically. Hydrogen atoms were placed in geometrically calculated positions and refined using a riding model. Images were created with the DIAMOND program [28]. In the structure of $\mathbf{1}\cdot CH_3OH$, a disorder was observed in the methanol molecule present as the solvent of crystallization.

3. Results and discussion

3.1. Synthesis

Complex $[Ru(PPh_3)_3Cl_2]$ was utilized as starting material during the synthesis of ruthenium complexes **1** and **2**. To synthesize complex $[Ru^{II}(L^1)(PPh_3)_2(CO)]$ (**1**), first the ligand L^1H_2 was deprotonated with sodium hydride (NaH) in dry dimethylformamide and then this deprotonated ligand was added to a hot methanolic solution of $Ru(PPh_3)_3Cl_2$. Prolonged heating (refluxing of 5–6 h) of this mixture afforded an orange colored solution of complex **1**. In case of complex $[Ru^{II}(L^3)(PPh_3)_2(DMF)]$ (**2**), the ligand L^2H_2 was added directly to $Ru(PPh_3)_3Cl_2$ in benzene–methanol mixture. Refluxing of this solution mixture for 5–6 h resulted in the formation of red colored solution. Red crystals of complex **2** were obtained after recrystallization of solution of **2** in dimethylformamide. Both the complexes **1** and **2** were highly soluble in most of the organic solvents such as dichloromethane, benzene, methanol and dimethylformamide. They were isolated in good yield and the synthetic procedures described above have been summarized in Scheme 3.

3.2. General properties

The infrared spectra of complexes **1** and **2** are shown in Fig. S1. IR spectrum of complex **1** revealed the presence of metal coordinated CO (carbon monoxide), as evidenced by CO stretching frequency (ν_{CO}) near 1936 cm^{-1} [29–33]. In addition to this, a band near 1672 cm^{-1} was observed due to the presence of carbonyl group of carboxamide moiety [12–14] in complex **1**. This IR band was found to be shifted to higher stretching frequency compared to the value of ν_{CO} observed in the free ligand (L^1H_2).

The IR spectrum of **2** did not display the characteristic band associated with C=O bond of carboxamide function which clearly indicated the conversion of ligand L^2H_2 during complex formation. A band near 1680 cm^{-1} was appeared in the infrared spectrum of complex **2** depicting the presence of metal coordinated dimethylformamide molecule in the complex. The peaks near 745 cm^{-1}, 695 cm^{-1} and 520 cm^{-1} were observed in both the complexes probably due to the presence of coordinated phosphine groups [34–36].

The electronic spectra of complexes **1** and **2** in dichloromethane and acetonitrile solutions are displayed in Fig. 1. The absorption bands with λ_{max} near 315 nm and 415 nm were observed in UV–vis spectrum of **1**. However, in case of complex **2**, these bands were observed with λ_{max} near 340 nm and 470 nm. The molar extinction coefficients of these bands indicate that they are of charge transfer type and probably due to metal to ligand charge (MLCT) transfer transition [32,37]. To observe the formation of a *solvento species*, the electronic

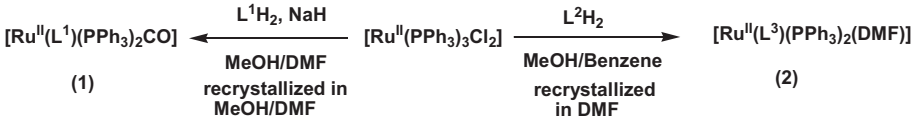

Scheme 3. Synthetic routes for ruthenium complexes **1** and **2**.

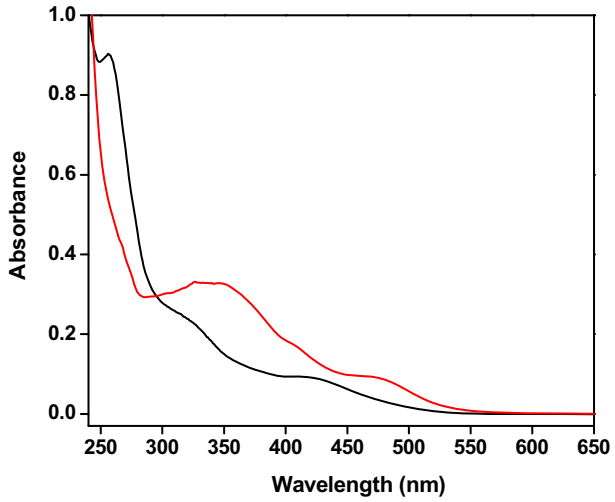

Fig. 1. Electronic absorption spectra of complexes **1** (black line) and **2** (red line) in dichloromethane and acetonitrile solutions respectively. (For interpretation of the references to color in this figure legend, the reader is referred to the web version of this article.)

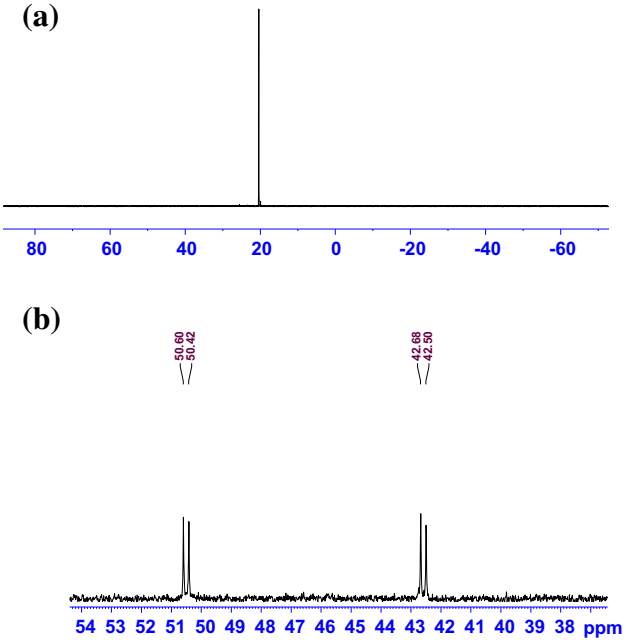

Fig. 2. ^{31}P NMR spectra of complexes (a) **1** and (b) **2** at room temperature.

spectrum of complex **2** was recorded in presence of different organic solvents. An absorption band near 470 nm (in acetonitrile) was red shifted to 495 nm in dimethylformamide solution. The same band was shifted to 505 nm in methanolic solution of **2** (Fig. S2).

^{1}H NMR spectra of ligands L^1H_2 and L^2H_2 were recorded in $(CD_3)_2SO$ solvent and the representative spectrum (the spectrum of L^2H_2) is shown in Fig. S3. All the expected multiple signals for aromatic protons were appeared in the range 7.0–8.5 ppm. In addition, the most deshielded singlet at ~11.5 ppm in ^{1}H NMR spectra of both the ligands was assigned to the proton of –CONH groups. Shaking their NMR sample solutions with D_2O depicted that the carboxamide proton was exchangeable [37] (Fig. S3(b)).

Complexes **1** and **2** were found to be diamagnetic which correspond to the bivalent state of ruthenium (low spin d^6, $S = 0$) in them. ^{1}H NMR and ^{31}P NMR spectra of **1** and **2** have been recorded in deuterated solvents. The expected multiple resonances for aromatic protons were observed within 6.5–8.5 ppm for both the complexes. A singlet at ~2.3 ppm in ^{1}H NMR spectrum of **1** exhibited the presence of six protons of two methyl groups in complex (Fig. S4). In case of complex **2**, two single resonances near 2.8 ppm and 2.9 ppm were observed for methyl protons of coordinated DMF (Fig. S5). The disappearance of singlet at ~11.0 ppm supported the absence of carboxamido proton in both the complexes **1** and **2**.

^{31}P NMR spectrum of complex **1** provided single peak at ~21.0 ppm which confirmed that two phosphine groups were at axial positions *trans* to each other (Fig. 2(a)) [15–17]. However ^{31}P NMR spectrum of **2** showed two double resonances of same intensities for phosphorus atoms at 50.60 ppm and 42.68 ppm (J_{PP} = 90 Hz) exhibiting the *cis* disposition of PPh_3 groups in complex **2** (shown in Fig. 2(b)) [38–40].

The ESI-mass spectra of complexes **1** and **2** were recorded in methanol and their experimental spectra along with the proposed fragmentation patterns have been displayed in Fig. S6 and Fig. S7 respectively. In the ESI-mass spectrum of complex **1**, the molecular ion peak corresponding to the neutral complex $[Ru(L^1)(PPh_3)_2(CO)]$ $(M)^+$ was detected at *m*/*z* 997.9 and the ion centered at *m*/*z* 736.0 was observed due to the presence of fragment $(M - PPh_3)^+$.

During the ESI-MS study of complex **2**, the molecular ion $(M)^+$ peak was not detected however a peak at *m*/*z* 1042.03 was appeared due to the presence of $[Ru(L^3)(PPh_3)_2]^+$ $(M - DMF)^+$ cationic species. During ESI process, the dissociation of DMF molecule probably took place due to the weak interaction between metal and the solvent molecule. Two peaks centered at *m*/*z* 780.11 and *m*/*z* 518.23 were also originated from the dissociation of two PPh_3 ligands from the coordination sphere of **2**.

3.3. Description of crystal structures

The molecular structures of complexes $[Ru(L^1)(PPh_3)_2(CO)]\cdot CH_3OH$ (**1**·CH_3OH) and $[Ru(L^3)(PPh_3)_2(DMF)]\cdot DMF$ (**2**·DMF) are shown in Figs. 3 and 4 and selected structural data has been listed in Tables 1 and 2 respectively.

In the crystal structure of **1**·CH_3OH, ruthenium center was found to be octahedrally coordinated having phosphine groups at

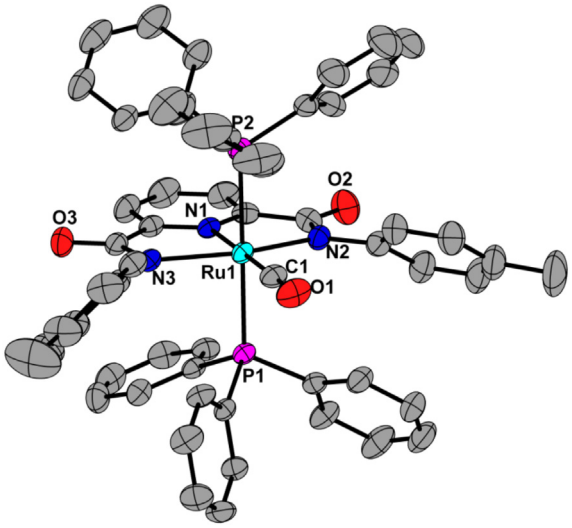

Fig. 3. ORTEP diagram (40% probability level) of complex $[Ru(L^1)(PPh_3)_2(CO)]\cdot CH_3OH$ (**1**·CH_3OH). All hydrogen atoms and solvent molecules are omitted for clarity.

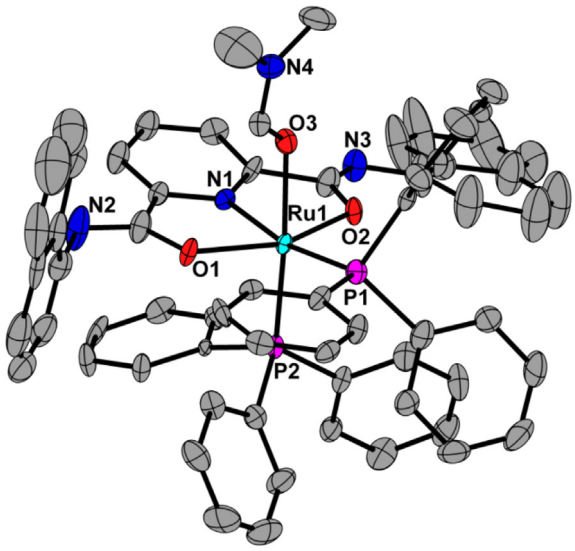

Fig. 4. ORTEP diagram (40% probability level) of complex $[Ru(L^3)(PPh_3)_2(DMF)]\cdot DMF$ (**2**·DMF). All hydrogen atoms and solvent molecules are omitted for clarity.

the axial positions *trans* to each other. One pyridine nitrogen (N1), two carboxamido nitrogens (N2 and N3) and C1 (CO) were found at equatorial positions in the structure. The distortion in octahedral geometry was also reflected in all the bond parameters around ruthenium center. In the molecular structure of **1**·CH_3OH, a disorder was observed in the methanol molecule present as the solvent of crystallization.

Interestingly, the structure of **1** showed that the carbon monoxide (CO) molecule was linearly coordinated to the ruthenium center (Ru–C–O angle ~177.5°). We did not provide any source of CO during the reaction. Dimethylformamide was the most probable source of CO which was utilized as the solvent in reaction mixture [41,42]. Ru–C(CO) [32,37,43,44], Ru–P [44,45], Ru–N(py) [46–48] and Ru–N(–CONH) [48] bond distances were found to be consistent with the reported values.

Table 1
Crystal data and structural refinement parameters for $[Ru(L^1)(PPh_3)_2(CO)]\cdot CH_3OH$ (**1**·CH_3OH) and $[Ru(L^3)(PPh_3)_2(DMF)]\cdot DMF$ (**2**·DMF).

	1·CH_3OH	**2**·DMF
Empirical formula	$C_{59}H_{51}N_3O_4P_2Ru$	$C_{69}H_{61}N_5O_4P_2Ru$
Formula weight (g mol^{-1})	1023.01	1187.24
Space group	*P* 21/c	*P* 21/c
Temperature/K	293(2)	293(2)
λ (Å) (Mo-Kα)	0.71073	0.71073
Crystal system	Monoclinic	Monoclinic
a (Å)	12.240(4)	13.076(2)
b (Å)	38.691(11)	25.048(4)
c (Å)	10.859(3)	20.783(3)
α (°)	90.00	90.00
β (°)	99.443(16)	121.638(7)
γ (°)	90.00	90.00
V (Å^3)	5073.0(3)	5795.4(16)
Z	4	4
ρ_{calc} (g cm^{-3})	1.339	1.361
Crystal size (mm)	0.32 × 0.25 × 0.20	0.23 × 0.19 × 0.16
F (000)	2108.0	2464.0
Theta range for data collection	2.17–25.00	1.41–28.32
Index ranges	$-14 < h < 13$, $-46 < k < 45$, $-12 < l < 12$	$-16 < h < 17$, $-33 < k < 32$, $-26 < l < 27$
Data/restraints/parameters	8935/0/625	14,446/230/716
GOF[a] on F^2	1.501	1.740
*R*1[b] [$I > 2\sigma(I)$]	0.0440	0.1780
*R*1[all data]	0.0685	0.2222
*wR*2[c] [$I > 2\sigma(I)$]	0.0664	0.1742
*wR*2 [all data]	0.0702	0.1829

[a] GOF = $[\Sigma[w(F_o^2 - F_c^2)^2]/M - N]^{1/2}$ (M = number of reflections, N = number of parameters refined).
[b] $R1 = \Sigma||F_o| - |F_c||/\Sigma|F_o|$.
[c] $wR2 = [\Sigma[w(F_o^2 - F_c^2)^2]/\Sigma[(F_o^2)^2]]^{1/2}$.

Table 2
Selected bond lengths (Å) and bond angles (°) for complexes $[Ru(L^1)(PPh_3)_2(CO)]\cdot CH_3OH$ (**1**·CH_3OH) and $[Ru(L^3)(PPh_3)_2(DMF)]\cdot DMF$ (**2**·DMF).

Bond lengths (Å)		Bond angles (°)	
2·DMF			
Ru(1)–O(1)	2.119(4)	N(1)–Ru(1)–P(1)	167.69(16)
Ru(1)–O(2)	2.115(4)	N(1)–Ru(1)–O(1)	77.8(2)
Ru(1)–N(1)	2.006(5)	N(1)–Ru(1)–O(2)	77.9(2)
Ru(1)–P(1)	2.3342(19)	O(3)–Ru(1)–P(2)	174.83(14)
Ru(1)–P(2)	2.262(2)	O(1)–Ru(1)–O(2)	155.48(17)
Ru(1)–O(3)	2.178(5)	O(3)–Ru(1)–O(2)	86.39(17)
O(3)–C(64)	1.255(8)	N(1)–Ru(1)–O(3)	80.07(19)
N(4)–C(64)	1.302(8)	P(1)–Ru(1)–P(2)	97.48(7)
1·CH_3OH			
Ru(1)–N(1)	2.047(2)	N(1)–Ru(1)–C(1)	178.98(11)
Ru(1)–N(2)	2.148(2)	N(1)–Ru(1)–N(2)	76.54(9)
Ru(1)–N(3)	2.150(2)	N(1)–Ru(1)–N(3)	76.94(9)
Ru(1)–P(1)	2.3903(9)	N(2)–Ru(1)–N(3)	153.33(9)
Ru(1)–P(2)	2.4708(10)	N(2)–Ru(1)–C(1)	102.89(12)
Ru(1)–C(1)	1.840(3)	P(1)–Ru(1)–C(1)	87.31(9)
C(1)–O(1)	1.161(3)	Ru(1)–C(1)–O(1)	177.5(3)
		P(1)–Ru(1)–P(2)	178.51(3)

The molecular structure of **2**·DMF also revealed several interesting aspects. The nitrogen atom from –CONH function of carboxamido ligand (L^2H_2) was not bound to ruthenium center however the enolate form (L^3) of this ligand was coordinated to the metal center through two oxygen atoms (O1 and O2) [1,34] and one pyridine nitrogen atom (N1). One phosphine group was observed at equatorial position *trans* to pyridine nitrogen (N1) whereas another PPh_3 group occupied an axial position *trans* to DMF molecule. Hence, a *cis* disposition of PPh_3 groups was found which was also supported by ^{31}P NMR data of **2**.

Ru–P [29,45] and Ru–N(py) [46–48] distances were found to be consistent to the reported values. Ru–P distances in the molecular structure of complex **2** (Ru–P1 = 2.3342(19) and Ru–P2 = 2.262(2)) were slightly smaller than that of values found in the structure of complex **1** (Ru–P1 = 2.3903(9) and Ru–P2 = 2.4708(10)).

The non-covalent interactions play an important role in the field of chemistry and biochemistry [49–51]. These weak interactions were found to be involved in the formation of crystal lattices of substances and this characteristic is often used as a promising approach in crystal engineering and supramolecular chemistry [49]. The interactions found in packing diagram of complex **2** are shown in Fig. S8. The intermolecular non-covalent interactions (C–H···π interactions) were observed between the naphthyl ring of one molecule and the phenyl hydrogen (PPh_3) of neighboring molecule in the packing diagram of complex **2**. The average distance between H43 and naphthyl ring was found nearly 2.48 Å.

3.4. Electrochemistry

We have investigated the redox properties of ruthenium center in complexes **1** and **2** by examining their dichloromethane solutions electrochemically using cyclic voltammetric studies. Cyclic voltammograms of both the complexes **1** and **2** showed single quasireversible redox couple with $E_{1/2}$ values near +0.82 V and +0.55 V versus Ag/AgCl respectively (Fig. 5). The peak to peak separation (ΔE_P) values for **1** and **2** were found near 97 mV and 70 mV. These data obtained from electrochemical studies clearly indicated the better stabilization of Ru(II) in complex **1** as compare

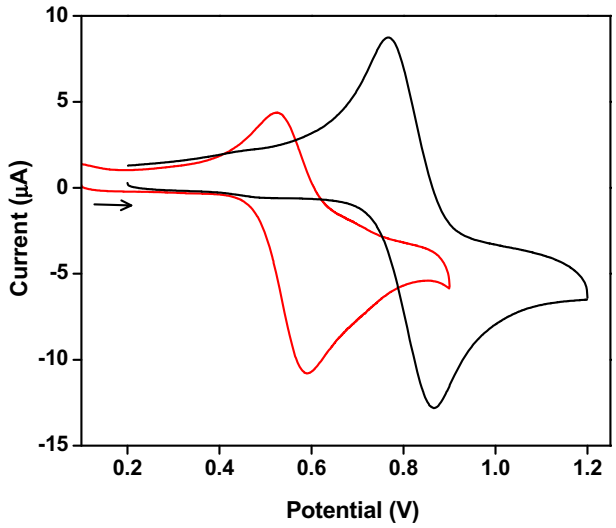

Fig. 5. Cyclic voltammograms of 10^{-3} M solutions of **1** (black line) and **2** (red line) in dichloromethane, in presence of 0.1 M tetrabutylammonium perchlorate (TBAP) using working electrode, glassy-carbon; reference electrode, Ag/AgCl; auxiliary electrode, platinum wire and scan rate, 0.1 V/s. (For interpretation of the references to color in this figure legend, the reader is referred to the web version of this article.)

to complex **2**. Both the responses found at positive potentials could be assigned to Ru(II)–Ru(III) couple [29,31,37] or could be due to the oxidation of the ligand containing non-innocent carboxamido ligand [3]. At this stage we were unable to isolate the oxidized product for both the complexes.

3.5. NO scavenging activity of ruthenium complexes

The use of transition metal complexes as nitric oxide scavengers was found to be an important approach to treat NO-mediated diseases [21–24,52–54]. In this endeavour, NO scavenging ability of complexes **1** and **2** was studied with Griess reagent assay by using UV–vis spectrophotometer. The electronic absorption spectra were taken in absence and in presence of complexes.

The production of nearly 24 μM of NO was detected when 25 μM aqueous solution of sodium nitrite was prepared in a 1 mL cuvette with 100 μL of the Griess reagent. The presence of 25 μM concentration of complex **1** in the same cuvette lowers the concentration of produced NO from 24 μM to 8.5 μM and the scavenging of nearly 15.5 μM of NO was observed (Fig. 6(a)). However complex **2** scavenged only around 7.0 μM of produced NO (Fig. 6(b)) even at the high concentration (100 μM).

Scavenging of NO by complexes **1** and **2** prompted us to investigate the mode of NO interaction in these complexes. We tried to understand the reaction pathways followed by **1** and **2** (Scheme S1) during nitric oxide scavenging studies, however we were unable to speculate any mechanism for the nitrosylation of complex **1**.

The formation of an orange–red complex was observed when a dichloromethane solution of complex **2** was reacted with *in situ* generated NO derived from acidified solution of sodium nitrite ($NaNO_2$). Sodium perchlorate ($NaClO_4$) with small amount of methanol was also added to the solution mixture to provide a counter anion. The resultant nitrosyl complex $[Ru(L^3)(PPh_3)_2(NO)](ClO_4)$ (**2a**) was characterized using infrared spectral study. IR spectrum of **2a** exhibited a band near 1880 cm^{-1} indicating the presence of $\{Ru–NO\}^6$ species in the complex (Fig. S9).

The IR peak near 1680 cm^{-1} (found in complex **2**) was disappeared which revealed the absence of metal coordinated DMF molecule in the complex. The presence of ClO_4^- ion as counter anion in the complex was also confirmed by observing the IR bands near 1090 cm^{-1} and 624 cm^{-1} [15–18].

4. Conclusions

In conclusion, we have synthesized two novel ruthenium(II) complexes $[Ru^{II}(L^1)(PPh_3)_2(CO)]$ (**1**) and $[Ru^{II}(L^3)(PPh_3)_2(DMF)]$ (**2**) derived from the ligands L^1H_2 and L^2H_2 respectively containing carboxamido nitrogen donors. The characterization of these complexes was performed by using IR, UV–vis and NMR spectral studies. ^1H and ^{31}P NMR spectral studies clearly depicted the bivalent state (low spin, d^6) of ruthenium center with $S = 0$ ground state in **1** and **2**. Complexes were characterized by ESI-MS studies and redox properties were investigated. Molecular structures of complexes **1** and **2** were determined using X-ray crystallographic studies. Crystal structure analysis of **2** revealed the conversion of ligand L^2H_2 (from keto to enol form) during complexation. Investigation of electrochemical studies indicated better stabilization of Ru(II) in complex **1** as compare to **2**. This higher stability of Ru(II) in complex **1** was observed due to the presence of metal coordinated CO which always stabilizes lower oxidation state of metal center. The NO scavenging activity of complexes **1** and **2** was also determined by Griess reagent. Complex **1** was found to be a better NO scavenger compared to complex **2**.

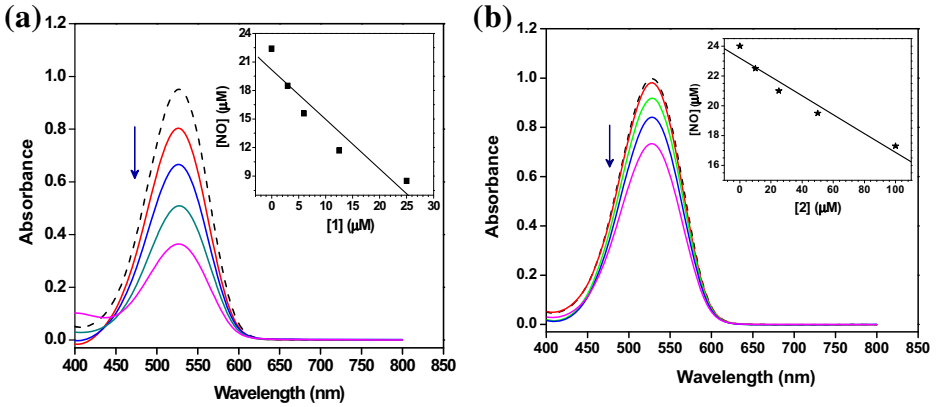

Fig. 6. Electronic spectra showing scavenging of NO in the presence of different concentrations of (a) complex **1** (0 μM–25 μM) and (b) complex **2** (10 μM–100 μM) in Griess assay (Griess reagent and sodium nitrite). Inset: changes in amount of dye formation with different concentrations of complexes in the presence of Griess reagent.

Acknowledgments

KG is thankful to CSIR, India for financial assistance No. 01(2720)/13/EMR-II dated 17-APRIL-2013). SK and RK are thankful to CSIR for financial support.

Appendix A. Supplementary data

Supplementary data related to this article can be found at http://dx.doi.org/10.1016/j.jorganchem.2013.10.054.

References

[1] K. Kamiya, M. Boero, K. Shiraishi, A. Oshiyama, J. Phys. Chem. B 110 (2006) 4443–4450.
[2] C. Panda, M. Ghosh, T. Panda, R. Banerjee, S.S. Gupta, Chem. Commun. 47 (2011) 8016–8018.
[3] A.K. Singh, V. Balamurugan, R. Mukherjee, Inorg. Chem. 42 (2003) 6497–6502.
[4] J.C. Noveron, M.M. Olmstead, P.K. Mascharak, Inorg. Chem. 37 (1998) 1138–1139.
[5] L.Q. Shen, E.S. Beach, Y. Xiang, D.J. Tshudy, N. Khanina, C.P. Horwitz, M.E. Bier, T.J. Collins, Environ. Sci. Technol. 45 (2011) 7882–7887.
[6] A. Chanda, D.-L. Popescu, F.T. de Oliveira, E.L. Bominaar, A.D. Ryabov, E. Munck, T.J. Collins, J. Inorg. Biochem. 100 (2006) 606–619.
[7] G.L. Millhauser, Acc. Chem. Res. 37 (2004) 79–85 and references therein.
[8] T.C. Harrop, P.K. Mascharak, Acc. Chem. Res. 37 (2004) 253–260.
[9] P.K. Mascharak, Coord. Chem. Rev. 225 (2002) 201–214.
[10] A. Miyanaga, S. Fushinobu, K. Ito, T. Wakagi, Biochem. Biophys. Res. Commun. 288 (2001) 1169–1174.
[11] M.J. Rose, P.K. Mascharak, Coord. Chem. Rev. 252 (2008) 2093–2114 and references therein.
[12] N.L. Fry, M.J. Rose, D.L. Rogow, C. Nyitray, M. Kaur, P.K. Mascharak, Inorg. Chem. 49 (2010) 1487–1495.
[13] A.K. Patra, M.J. Rose, K.A. Murphy, M.M. Olmstead, P.K. Mascharak, Inorg. Chem. 43 (2004) 4487–4495.
[14] N.L. Fry, B.J. Heilman, P.K. Mascharak, Inorg. Chem. 50 (2011) 317–324.
[15] K. Ghosh, S. Kumar, R. Kumar, U.P. Singh, Eur. J. Inorg. Chem. (2012) 929–938.
[16] K. Ghosh, S. Kumar, R. Kumar, U.P. Singh, N. Goel, Organometallics 30 (2011) 2498–2505.
[17] K. Ghosh, S. Kumar, R. Kumar, U.P. Singh, N. Goel, Inorg. Chem. 49 (2010) 7235–7237.
[18] K. Ghosh, R. Kumar, S. Kumar, J.S. Meena, Dalton Trans. 42 (2013) 13444–13452.
[19] K. Ghosh, S. Kumar, R. Kumar, Inorg. Chem. Commun. 14 (2011) 146–149.
[20] K. Ghosh, S. Kumar, R. Kumar, Inorg. Chim. Acta 405 (2013) 24–30.
[21] D.A. Riccio, M.H. Schoenfisch, Coord. Soc. Rev. 41 (2012) 3731–3741.
[22] A.W. Carpenter, M.H. Schoenfisch, Coord. Soc. Rev. 41 (2012) 3742–3752.
[23] T.S. Kamatchi, N. Chitrapriya, H. Lee, C.F. Fronczek, F.R. Fronczek, K. Natarajan, Dalton Trans. 41 (2012) 2066–2077.
[24] H. Subedi, N.E. Brasch, Inorg. Chem. 52 (2013) 11608–11617.
[25] J.A. Cowan, Inorganic Biochemistry: an Introduction, VCH Publication, New York, 1993, p. 7.
[26] G.M. Sheldrick, Acta Crystallogr. A46 (1990) 467–473.
[27] G.M. Sheldrick, "SHELXTL-NT 2000" Version 6.12, Reference Manual, University of Gottingen, Pergamon, New York, 1980.
[28] B. Klaus, "Diamond" Version 1.2c, University of Bonn, Germany, 1999.
[29] K.N. Kumar, R. Ramesh, Y. Liu, J. Inorg. Biochem. 100 (2006) 18–26.
[30] K.N. Kumar, R. Ramesh, Y. Liu, Mol. Catal. A Chem. 265 (2007) 218–226.
[31] C. GuhaRoy, S.S. Sen, S. Dutta, G. Mostafa, S. Bhattacharya, Polyhedron 26 (2007) 3876–3884.
[32] B.K. Panda, S. Chattopadhyay, K. Ghosh, A. Chakravorty, Organometallics 21 (2002) 2773–2780.
[33] M.A. Gonzalez, N.L. Fry, R. Burt, R. Davda, A. Hobbs, P.K. Mascharak, Inorg. Chem. 50 (2011) 3127–3134.
[34] R. Raveendran, S. Pal, J. Organomet. Chem. 694 (2009) 1482–1486.
[35] P. Munshi, R. Samanta, G.K. Lahiri, J. Organomet. Chem. 586 (1999) 176–183.
[36] G.K. Lahiri, S. Bhattacharya, M. Mukherjee, A.K. Mukherjee, A. Chakravorty, Inorg. Chem. 26 (1987) 3359–3365.
[37] K. Ghosh, S. Pattanayak, A. Chakravorty, Organometallics 17 (1998) 1956–1960.
[38] A.R. Naziruddin, A. Hepp, T. Pape, F.E. Hahn, Organometallics 30 (2011) 5859–5866.
[39] P. Jaunky, H.W. Schmalle, M. Alfonso, T. Fox, H. Berke, J. Organomet. Chem. 689 (2004) 801–810.
[40] E. Valls, J. Suades, R. Mathieu, Organometallics 18 (1999) 5475–5483.
[41] Y. Wan, M. Alterman, M. Larhed, A. Hallberg, J. Org. Chem. 67 (2002) 6232–6235.
[42] D. Hesek, M. Lee, B.C. Noll, J.F. Fisher, S. Mobashery, J. Org. Chem. 74 (2009) 2567–2570.
[43] K. Ghosh, S. Chattopadhyay, S. Pattanayak, A. Chakravorty, Organometallics 20 (2001) 1419–1423.
[44] S.A. Moya, M. Vidal, G. Abarca, C. Martinez, V. Guerchais, H. Le Bozec, M.T. Garland, S. Rodriguez, P. Aguirre, Inorg. Chem. Commun. 13 (2010) 1519–1521.
[45] N. Chitrapriya, V. Mahalingam, M. Zeller, K. Natarajan, Polyhedron 27 (2008) 1573–1580.
[46] N. Chanda, S.M. Mobin, V.G. Puranik, A. Datta, M. Niemeyer, G.K. Lahiri, Inorg. Chem. 43 (2004) 1056–1064.
[47] S. Khatua, D. Samanta, J.W. Bats, M. Schmittel, Inorg. Chem. 51 (2012) 7075–7086.
[48] M. Dasgupta, S. Nag, G. Das, M. Nethaji, S. Bhattacharya, Polyhedron 27 (2008) 139–150.
[49] G.R. Desiraju, T. Steiner, The Weak Hydrogen Bond in Structural Chemistry and Biology, Oxford University Press, New York, 1999.
[50] A. Nangia, J. Chem. Sci. 122 (2010) 295–310.
[51] R.R. Knowles, E.N. Jacobsen, Proc. Natl. Acad. Sci. U.S.A. 107 (2010) 20678–20685.
[52] B.R. Cameron, M.C. Darkes, H. Yee, M. Olsen, S.P. Fricker, R.T. Skerlj, G.J. Bridger, N.A. Davies, M.T. Wilson, D.J. Rose, J. Zubieta, Inorg. Chem. 42 (2003) 1868–1876.
[53] S.P. Fricker, Platin. Met. Rev. 39 (1995) 150–159.
[54] C.J. Marmion, B. Cameron, C. Mulcahy, S.P. Fricker, Curr. Top. Med. Chem. 4 (2004) 1585–1603.